Journal of chemical & engineering data

Article

pubs.acs.org/jced

Measurement and Modeling of Adsorption of Lower Hydrocarbons on Activated Carbon

Gouri Shankar Cheripally, Ashok Mannava, Gaurav Kumar, Rakeshroshan Gupta, Prabirkumar Saha, Bishnupada Mandal, Ramgopal Uppaluri, Sasidhar Gumma, and Aloke Kumar Ghoshal*

Department of Chemical Engineering, Indian Institute of Technology, Guwahati, India

Supporting Information

ABSTRACT: This work reports adsorption isotherms for C_1 to C_6 hydrocarbons on activated carbon at three different temperatures (293 K, 318 K, and 358 K) over a wide range of pressure (0 bar to 100 bar). The isotherms were measured using a standard gravimetric method. The experimental data were correlated and compared using Toth, modified virial, and potential theory models. On the basis of the adsorption potential, characteristic curves were also generated for methane, ethane, propane, isobutane, *n*-pentane, and *n*-hexane on activated carbon over broad ranges of pressure and temperatures. The micropore volume of the activated carbon predicted from potential theory was in good agreement with those obtained using a N_2 isotherm measured at 77 K. The enthalpy of adsorption at zero loading was found to increase linearly with the carbon number.

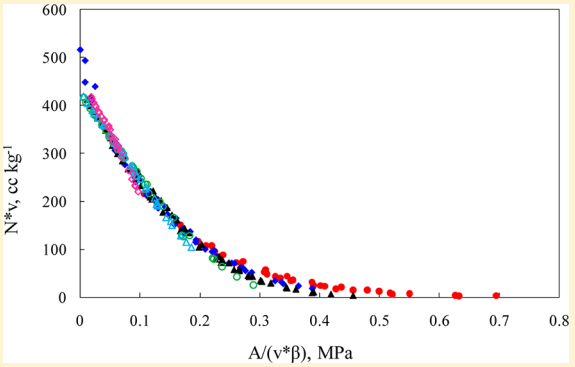

1. INTRODUCTION

Industrial separation of hydrocarbon gaseous mixtures is of importance in the oil and gas industries. Apart from pressure swing and thermal swing adsorption processes[1,2] adsorptive natural gas storage has also been widely studied.[3] Applicability of adsorptive technologies in such cases requires knowledge of adsorption equilibria over wide pressure and temperature range. Adsorption data for hydrocarbons (C_1 to C_6) up to very high pressures on activated carbon are comparatively scarce in literature. Grant et al.[4] gravimetrically measured adsorption isotherms of normal paraffins and sulfur compounds on activated carbon. Subsequently, the data were correlated using modified potential theory proposed by Lewis et al.[5] Single and multicomponent adsorption equilibria of lower hydrocarbons and CO_2 (up to about 35 bar) were presented by Reich et al.[6] Subsequently, potential theory was applied to predict multicomponent adsorption equilibria. Herden et al.[7] measured equilibria for C_1 to C_4 paraffins at low temperatures and pressures up to 1 bar on different activated carbon samples; they have evaluated parameters for the Dubinin−Radushkevich model. Mayfield et al.[8] measured the adsorption equilibria and kinetics of hydrocarbons (ethane, butane, and pentane) on commercially available activated carbon Ajax using a differential adsorption bed. Malek et al.[9] measured equilibrium isotherms of methane, ethane, and propane on activated carbon and silica gel using dynamic column breakthrough and constant flow equilibrium desorption methods. They found that both methods were very effective for measuring single component adsorption data. Holland et al.[10] determined adsorption isotherms for C_1−C_7 normal alkanes on activated carbon by gravimetric measurement and correlated the data using a stepwise statistically optimized model to evaluate thermodynamic properties.[11] Recently, Zhu et al.[12] measured isotherms for lower alkanes and alkenes on Kuerha-activated carbon.

Adsorption equilibrium for hydrocarbons over wider ranges of operating conditions is necessary to characterize adsorbent surfaces and evaluate thermodynamic properties through adsorption modeling for applications such as natural gas storage. Moreover, models such as IAST, that predict binary adsorption characteristics of a solid adsorbent often necessitate knowledge of adsorption capacity of lighter components to high pressures.[13] While pure component isotherm models may be used to estimate adsorption at higher pressures through extrapolations, their validity is not guaranteed.

The principal objective of this work is to measure adsorption capacities of an activated carbon, and model the experimental adsorption data for C_1−C_6 hydrocarbons. Adsorption isotherms of hydrocarbons (methane, ethane, propane, isobutane, *n*-pentane, and *n*-hexane) on activated carbon were measured gravimetrically on a magnetic suspension balance over wide ranges of temperatures (293 K to 358 K) and pressures. While adsorption of lower hydrocarbons on activated carbon is well reported in the literature, data over wide range of temperatures and at high pressures as reported in this work are scare. Another objective of the work is to correlate the adsorption data over the wide pressure range with a suitable yet simple isotherm model. Toth, modified virial, and potential theory based models were used to correlate the experimental data.

Received: December 13, 2012
Accepted: April 25, 2013
Published: May 9, 2013

2. EXPERIMENTAL SECTION

2.1. Materials. Helium (99.99%), methane (99.95%), ethane (99.5%), propane (99.5%), and isobutane (99.5%) are supplied by Vadilal Industries Ltd., Ahmedabad, India. Extra pure analytical grade *n*-pentane and *n*-hexane obtained from Merck were used directly without any further treatment. Commercial activated carbon adsorbent of grade RV950G as cylindrical pellets of 2 to 4 mm size is obtained from R.V. Corporation, Mumbai, India. The starting material for this activated carbon is coconut shell. Because of the coconut shell, activated carbon pellets have very high hardness and low attrition losses; because of the high hardness, these activated carbon granules are especially suitable for high pressure applications.

2.2. Characterization of Activated Carbon. Pore volume, pore size distribution (PSD), and BET surface area of activated carbon were measured using nitrogen at 77 K in a surface area and pore size analyzer (Coulter SA 3100). Figure 1

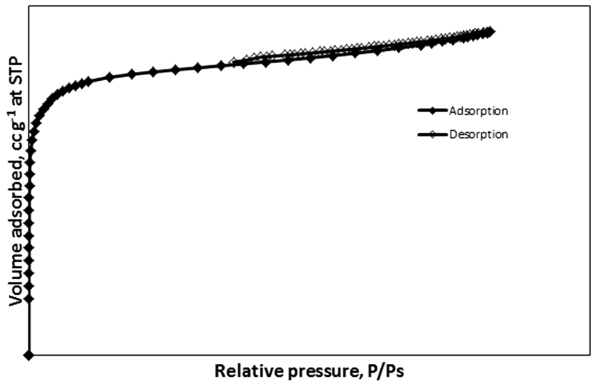

Figure 1. N_2 adsorption and desorption at 77 K.

depicts this adsorption isotherm and the properties which are summarized in Table 1.

Table 1. Physical Properties of Activated Carbon

	this work	Holland et al.[10]
BET surface area/m^2 g^{-1}	849	1251
micropore surface area/m^2 g^{-1}	668	N/A
total pore volume/cm^3 g^{-1}	0.429	0.799
micropore volume/cm^3 g^{-1}	0.296	N/A

2.3. Isotherm Measurements. Adsorption equilibria of methane, ethane, propane, isobutane, *n*-pentane and *n*-hexane on activated carbon were measured gravimetrically using a Rubotherm magnetic suspension balance at temperatures 293 K, 318 K, and 358 K and over wide range of pressures (up to high pressures).

In a typical adsorption experiment, about 2 g of an activated carbon sample was loaded in the sample holder and was activated at 473 K for more than 12 h. During activation, helium was allowed to flow over the sample at 20 cm^3 min^{-1} under vacuum. After activation, the sample was cooled down to the desired experimental temperature and the chamber was completely evacuated. After desired temperature was established in the system, a gas of interest (C_1 to C_6 hydrocarbons) was introduced to the desired experimental pressure and sufficient time was allowed for equilibrium to measure the adsorption capacity. Equilibrium was assumed when change in sample weight in 30 min was less than 0.1 mg. The next point was measured by incrementally charging the equilibrium cell with the gas to the desired pressure. After completing one isotherm measurement, the sample was thoroughly activated to prepare it for measurement of the next isotherm. Usual buoyancy correction[13−15] was made to obtain the excess amount adsorbed. This step involved measurement of the buoyancy effect of helium on the bucket and sample assembly at room temperature.

3. ISOTHERMS

Adsorption isotherms for various hydrocarbons are represented in terms of fugacity (f, bar) and excess amount adsorbed (N, mmol g^{-1} at STP), following suggested procedure in literature to report adsorption data at such high pressures.[13] The fugacity at the given equilibrium conditions was calculated using Peng−Robinson EoS. The adsorption isotherms of methane, ethane, propane, isobutane, *n*-pentane, and *n*-hexane at three different temperatures (293, 318, and 358 K) are given in Figure 2. Figure 3 shows the adsorption isotherms of the C_1 to C_6 hydrocarbons at 358 K up to 2 bar. The loading of CH_4 and C_2H_6 obtained in this work are comparable to those reported on Brazilian coconut shells and coconut nanoporous activated carbon by Walton et al.[16,17] The isotherms of all hydrocarbons (C_1−C_6) are also similar to those reported by Herden et al.[7] and Mayfield et al.[8] on activated carbon. As expected, the Henry's constant (initial slope of the isotherm in Figure 3) increases with carbon number of the adsorbate. This is mainly due to increase in polarizability of the gas molecules. The capacities for methane, ethane, propane, *n*-pentane, and *n*-hexane at 293 K in the low pressure region (up to a relative pressure of about 0.01) obtained in this work were slightly higher than those reported by Holland et al.[10] (Figure 4). However in the high pressure region, the capacities (especially for pentane and hexane) reported by Holland et al.[10] were higher. This difference is due to a difference in pore size and surface areas of the two samples; the surface area and pore volume of the adsorbent used in the work by Holland et al.[10] was about 1251 m^2 g^{-1} and 0.799 cm^3 g m^{-1} respectively, which is widely different from the sample used in this work (Table 1).

4. ISOTHERM MODELING

A simple yet accurate isotherm model is essential to describe the single component adsorption isotherms and to characterize the adsorbent. The isotherm models are often necessary for analysis of the adsorption characteristics on the adsorbent and design of any process. While the accuracy of the models generally depends upon the independent parameters present in the equation, models with more independent parameters tend to aggrandize numerical complexity. In this work, we have used modified virial model and Toth model to fit the experimental data for adsorption of hydrocarbon gases studied. In addition, an attempt is made to use a single characteristic curve to describe adsorption of all the adsorbates considered in the work; challenges involved in modeling the entire data over wide range of temperature and pressures are discussed.

Toth equation fulfills the both end limits of isotherm and hence is one of the widely used empirical models to represent adsorption data on heterogeneous adsorbents. The model is often represented in the following form:[18,19]

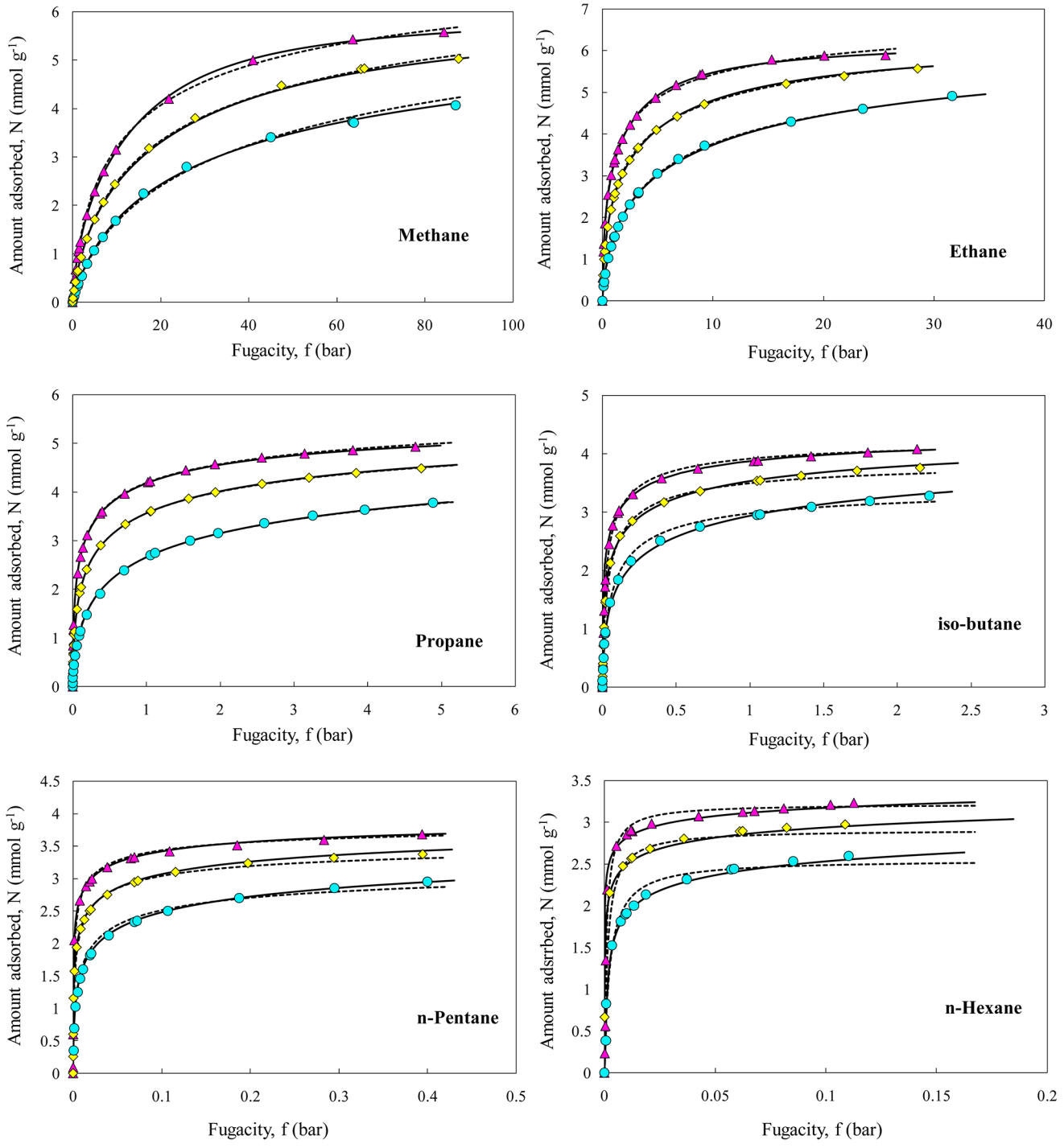

Figure 2. Isotherms of hydrocarbons on activated carbon. Experimental data at ▲, 293 K; ♦, 318 K; and ●, 358 K; lines (solid for modified virial isotherm and dashed for Toth isotherms) are fits using model parameters from Table 2.

$$\frac{N}{N_m} = \frac{b^{1/n} f}{(1 + bf^n)^{1/n}} \quad (1)$$

$$b = b^{(0)} \exp(b^{(1)}/T) \quad (2)$$

where, N and N_m represent the amount adsorbed per unit mass of adsorbent (mmol g^{-1}) and saturation capacity (mmol g^{-1}) respectively, f is the fugacity in bar, n, b (bar^{-n}), b_o (bar^{-n}), and b_1 (K) are the constants that are specific for particular adsorbate−adsorbent system. However, due to the wide temperature range used in this study, a single value of saturation loading was not applicable to all temperatures to some of the gases. In such cases, the temperature dependency of saturation loading was described using the functionality[20]

$$N_m = N_m^{(0)} \exp(N_m^{(1)}/T) \quad (3)$$

Table 2 presents parameters estimated for the Toth equation using hydrocarbon adsorption data. The values of n are in the range of 0.36 to 0.98 indicating the presence of heterogeneity of the adsorbent surface. The fits for this model are also shown in Figure 2 along with the experimental data.

dx.doi.org/10.1021/je3013217 | J. Chem. Eng. Data 2013, 58, 1606−1612

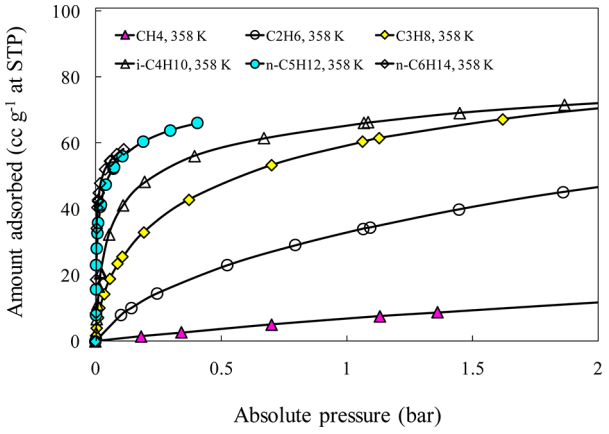

Figure 3. Adsorption isotherms of different hydrocarbons onto activated carbon at 358 K up to 2 bar. Points are experimental data and lines are drawn as guide to the eye.

4.1. Modified Virial. The modified virial model is presented as follows[21]

$$\ln\left(\frac{f}{N}\right) = \frac{1}{H}\left(\frac{N_m}{N_m - N}\right) \times \exp\left[\left(C_{10} + \frac{C_{11}}{T}\right)N + \left(C_{20} + \frac{C_{21}}{T}\right)N^2\right] \quad (4)$$

where f is the fugacity in bar, N_m is the saturation loading in mmol g^{-1}, T is the temperature in K and Cs are the virial coefficients. The temperature dependency of Henry's constant H is given by

$$H = H_o \exp(-H_1/T) \quad (5)$$

The model is a modified form of virial equation, which is versatile and can represent a wide variety of isotherms and can also account for saturation at high pressures. In addition, it also accounts for saturation at high loadings as in case of a Langmuir equation. The fits for this model are also shown in Figure 2, and the experimental data and parameters are given in Table 2.

4.2. Characteristic Curve from Potential Theory. According to the potential theory, the adsorbed amount can be related to the adsorption potential through

$$Nv = f\left\{\frac{A}{\beta v}\right\} \quad (6)$$

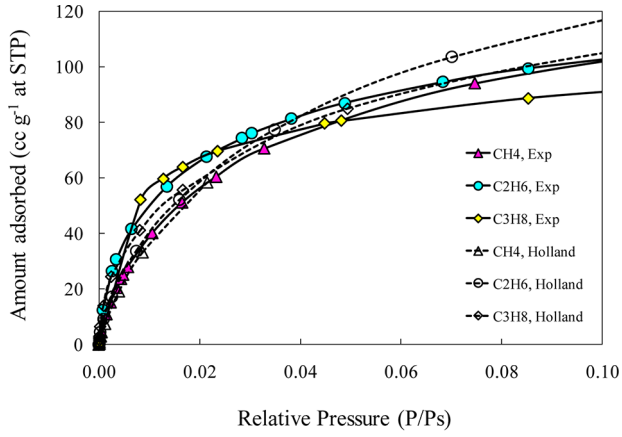

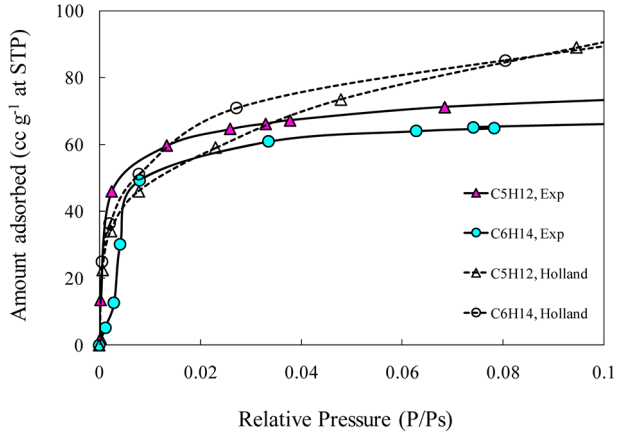

Figure 4. Comparison of adsorption isotherms of hydrocarbons on activated carbon at 293 K. Continuous line and dashed lines represent experimental data on activated carbon with surface area 849 m^2 g^{-1} and literature (Holland et al.[7,10]) data with surface area 1251 m^2 g^{-1}, respectively.

where N is the amount adsorbed (mmol g^{-1}), v is molar volume of the adsorbed phase, A is the adsorption potential, and β is the similarity coefficient. The adsorption potential A is commonly given by the following expression in literature.

$$A = RT \ln\left(\frac{P^s}{P}\right) \quad (7)$$

Table 2. Isotherm Model Parameters Estimated from Toth and Modified Virial Models

parameter	methane	ethane	propane	isobutane	pentane	hexane
			Toth			
N_m^0/mol kg^{-1}	7.68	7.35	6.40	1.41	1.69	0.89
N_m^1/K	0.00	0.00	0.00	327.65	250.26	375.33
b_0/bar^{-n}	0.006	0.0163	0.070	0.689	0.562	5.710
b_1/K	−1239.3	−1426.0	−1309.5	−913.4	−1270.3	−1478.1
n	0.572	0.480	0.354	0.642	0.429	0.978
			Modified Virial			
C_{10}/kg mol^{-1}	0.748	−0.078	0.587	0.262	0.930	0.454
C_{11}/mol^{-1} kg K	351.12	152.83	30.45	235.78	−14.90	−811.41
C_{20}/kg^2 mol^{-2}	0.251	0.050			0.100	0.251
C_{21}/kg^2 mol^{-2} K	−91.92	−28.30			21.43	257.35
H_1/K	−2309.6	−3141.5	−3748.4	−4507.4	−5204.7	−5656.85
$H_o \times 10^3$, mol kg^{-1} bar^{-1}	0.544	0.629	0.879	0.464	0.799	0.058
N_m, mol kg^{-1}	6.05	6.27	5.487	4.33	3.91	3.62
			Potential Theory Model			
β	0.93	0.97	1	0.98	1.16	1.57

dx.doi.org/10.1021/je3013217 | J. Chem. Eng. Data 2013, 58, 1606−1612

where P^s and P are the vapor pressure and equilibrium of the adsorbate at the equilibrium temperature T. However, due to the wide range of pressures used in this work, we replace pressure with fugacities for defining the adsorption potential[5]

$$A = RT \ln\left(\frac{f^s}{f}\right) \tag{8}$$

As is the convention we extrapolated the vapor pressure curve to obtain P^s (and f^s) at $T > T_c$. Usually, molar volume of the adsorbate is considered to be a constant (equal to liquid volume at its normal boiling point) or some temperature dependency is considered to account for the change in liquid volume with temperature. Using molar volume of adsorbate at its normal boiling point resulted in a characteristic curve with a large scatter especially at high loading (Figure 5a). This is due to the wide temperature and pressure range we have considered in this work. To overcome the problem, we chose to follow the procedure suggested by Lewis et al.[5] The molar volume of the adsorbate is considered to be equal to that of the liquid in equilibrium with vapor at the equilibrium pressure (and appropriate temperature). By making this modification, we obtained the characteristic curve shown in Figure 5b.

To superimpose all adsorbate curves, propane was taken as reference ($\beta = 1$) and β for other hydrocarbons were calculated by a curve fitting method. The resultant characteristic curve is given in Figure 5c and the values for similar coefficients are given in Table 2. The best fit equation to describe the characteristic equation is given by the following exponential function

$$Nv = 430 \exp\left[-10.05\left(\frac{A}{\beta v}\right)^{1.24}\right] \tag{9}$$

In the above expression, N is in mmol g^{-1}, v is in cc mol^{-1}, and A is in J mol^{-1} the constant 430 (cc kg^{-1}) represents limiting volume of adsorption and an exponent value of 1.24 is dependent upon the micropore system. In the original formulation, the value of the power is 2, and its reduction to 1.24 suggests an increase in the heterogeneity of the micropore system.[22] It can also be observed that the limiting volume of adsorption obtained here matches well with the micropore volume of 0.429 cc g^{-1} obtained from N_2 isotherm at 77 K.

Several efforts were made to describe data for methane at $P > P_c$ following suggested methods for adsorption at supercritical conditions.[23] However, we were unsuccessful to superimpose the data obtained in this work at supercritical conditions on the resultant characteristic curve using any of the methods. In addition, some deviation at high pressures ($P/P_c > 0.5$) was also observed for ethane (Figure 5). This was in agreement with the observations of Reich et al.[6] who reported the inability of potential theory to predict data at temperatures above critical temperatures. However, the potential theory provided good results at other conditions for these two adsorbates also.

5. ENTHALPY OF ADSORPTION

The enthalpy of adsorption is useful in the characterization of adsorbent−adsorbate system. It can be calculated at constant adsorbate concentration using the expression[20]

$$\Delta h_{ads} = -R\left.\frac{\partial(\ln f)}{\partial(1/T)}\right|_N \tag{10}$$

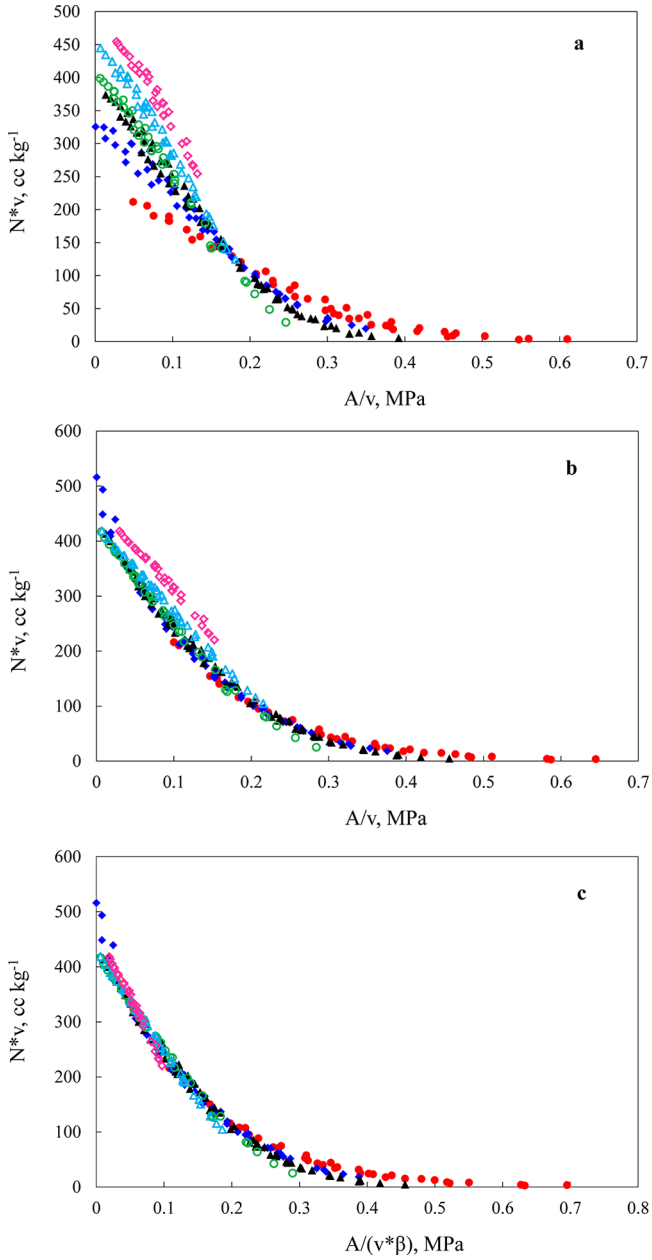

Figure 5. Characteristic curve for ●, methane; ♦, ethane, ▲, propane, ○, isobutene, △, *n*-pentane, and ◊, *n*-hexane on activated carbon at 293 K, 318 K, and 358 K: (a) v is liquid molar volume at normal boiling point; (b) v is liquid molar volume at vapor pressure equal to equilibrium pressure; (c) characteristics curve after including similarity coefficient (β) in abscissa.

where, Δh_{ads} is enthalpy of adsorption (J mol^{-1}), P is the equilibrium pressure, T is temperature (K), N is amount adsorbed (mmol g^{-1}), and R is gas constant (J mol^{-1} K^{-1}).

According to the Langmuir model, the enthalpy of adsorption should be independent of coverage, but this requirement is rarely fulfilled in real systems. This is due to the role of surface heterogeneity and adsorbate−adsorbate interaction under such circumstances.[20]

Usually, the enthalpy of adsorption alters with surface coverage and is useful to characterize the heterogeneity of the surface structure. For homogeneous surfaces, with an increase in the coverage, the enthalpy of adsorption increases because of enhancement in lateral interactions. A reduction in enthalpy of

dx.doi.org/10.1021/je3013217 | J. Chem. Eng. Data 2013, 58, 1606−1612

adsorption with increasing surface coverage usually indicates the heterogeneity of the adsorbent. However, a constant value does not necessarily indicate the homogeneity of the adsorbent as it could be due to the combined effect of decrease in vertical interactions and near equal increase in the lateral interactions.

The variation of adsorption enthalpy with loading using modified virial model is given in Figure 6a. At zero loading, the

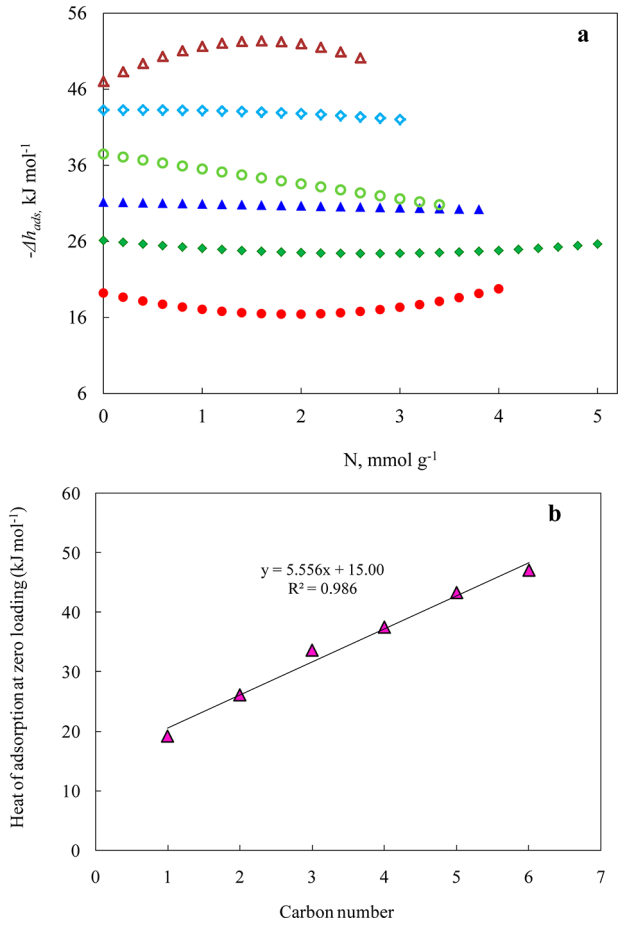

Figure 6. (a) Variation of adsorption enthalpy with loading for ●, methane; ♦, ethane, ▲, propane, ○, isobutene, ◊, *n*-pentane, and △, *n*-hexane. (b) Variation of enthalpy of adsorption at zero loading with carbon number.

enthalpies of adsorption for C_1 to C_6 hydrocarbons are found to increase with carbon number as shown in Figure 6b. This was expected as the polarizability increases with carbon number and hence the strength of lateral interactions increases.

For methane, there is a decrease in enthalpy of adsorption with loading initially; but as loading increases, lateral interactions become significant and enthalpy starts to increase. With an increase in carbon number, the strength of lateral interactions also increases and the enthalpy–loading curves become flatter. In fact for *n*-hexane, the increase in lateral interactions is high enough to compensate the decrease the vertical interactions and hence the enthalpy increases with loading initially. The exception to this trend is in the case of isobutane where a significant decrease occurs in the vertical interactions and lateral interactions are not strong enough to compensate for this decrease; one reason for this difference in behavior of isobutane may be due to its significantly larger kinetic diameter (0.5 nm) compared to all the other adsorbates.

6. CONCLUSIONS

Adsorption isotherms of methane, ethane, propane, isobutane, *n*-pentane, and *n*-hexane on activated carbon were measured gravimetrically at three temperatures 293 K, 318 K, and 358 K over a wide range of pressures. Adsorption capacities were observed to increase with carbon number. The experimental single component adsorption data were correlated using Toth, modified virial, and potential theory models. The heterogeneity of the system is indicated by the value of *n* in the Toth model. The potential theory was used to generate the characteristic curve, to predict the single component adsorption loading on the given material. In generating the characterstic curve, molar volumes for the adsorbate were assumed to be equal to that of saturated liquid with vapor pressure equal to that of the equilibrium adsorption pressure. However, the potential theory was unable to describe the data at very high pressures for methane and ethane.

The enthalpies of adsorption at zero loading were found to increase linearly with the carbon number as expected. With an increase in loading, an increase in lateral interactions significantly offsets the decrease in vertical interactions for all gases studied with the exception of isobutane. For isobutane the decrease in vertical interactions is higher than in case of other hydrocarbons possibly due to its larger kinetic diameter.

■ ASSOCIATED CONTENT

Ⓢ Supporting Information

Methane, ethane, propane, isobutene, *n*-pentane, and *n*-hexane adsorption on activated carbon data. This material is available free of charge via the Internet at http://pubs.acs.org.

■ AUTHOR INFORMATION

Corresponding Author

*Tel.: +91 361 2582252. Fax: +91 361 2582291. E-mail: aloke@iitg.ernet.in.

Funding

We gratefully acknowledge Oil India Limited, Duliajan, for financial support to carry out this research work.

Notes

The authors declare no competing financial interest.

■ REFERENCES

(1) Ruthven, D. M. *Principles of Adsorption and Adsorption Process*; Wiley: New York, 1984.
(2) Yang, R. T. *Gas Separation by Adsorption Processes*; Imperial College Press: Boston, 1997; Vol. *1*.
(3) Sircar, S.; Golden, T. C.; Rao, M. B. Activated Carbon for Gas Separation and Storage. *Carbon* **1996**, *34*, 1.
(4) Grant, R. J.; Manes, M.; Smith, S. B. Adsorption of Normal Paraffins and Sulfur Compounds on Activated Carbon. *AIChE J.* **1962**, *8*, 403.
(5) Lewis, W. K.; Gilliland, E. R.; Chertow; Cadogan, W. P. Pure Gas Isotherms. *Ind. Eng. Chem.* **1950**, *42*, 1326.
(6) Reich, R.; Ziegler, W. T.; Rogers, K. A. Adsorption of Methane, Ethane, and Ethylene Gases and their Binary and Ternary Mixtures and Carbon Dioxide on Activated Carbon at 212–301 K and Pressures to 35 atm. *Ind. Eng. Chem. Process Des. Dev.* **1980**, *19*, 336.
(7) Herden, H.; Loffler, U.; Schollner, R. Adsorption of Hydrocarbons on Activated Carbon. *J. Colloid Interface Sci.* **1991**, *144*, 477.
(8) Mayfield, P. L. J.; Do, D. D. Measurement of the Single Component Adsorption Kinetics of Ethane, Butane and Pentane onto Activated Carbon Using Differential Adsorption Bed. *Ind. Eng. Chem. Res.* **1991**, *30*, 1262.

(9) Malek, A.; Farooq, S. Determination of Equilibrium Isotherms Using Dynamic coloumn Breakthrough and Constant Flow Equilibrium Desorption. *J. Chem. Eng. Data* **1996**, *41*, 32.
(10) Holland, C.E..; Al-Muhtaseb, S. A.; Ritter, J. A. Adsorption of C_1−C_7 Normal Alkanes on BAX Activated Carbon. 1. Potential Theory Correlation and Adsorbent Characterization. *Ind. Eng. Chem. Res.* **2001**, *40*, 338.
(11) Al-Muhtaseb, S. A.; Holland, C.E..; Ritter, J. A. Adsorption of C1−C7 Normal Alkanes on BAX Activated Carbon. 2. Statistically Optimized Approach for Deriving Thermodynamic Properties from the Adsorption Isotherm. *Ind. Eng. Chem. Res.* **2001**, *40*, 319.
(12) Zhu, W.; Groen, J. C.; Miltenburg, A. V.; Kapteijn, F.; Moulijn, J. N. Comparision of Adsorption Behavior of Light Alkanes and Alkenes on Kureha Activated Carbon. *Carbon* **2005**, *43*, 1416.
(13) Talu, O. Needs, Status, Techniques and Problems with Binary Gas Adsorption Experiments. *J. Colloid Interface Sci.* **1998**, *76*−*77*, 227.
(14) Keller, J.; Staudt, R. *Gas Adsorption Equilibria, Experimental Methods and Adsorptive Isotherms*; Springer: New York, 2005.
(15) Vermesse, J.; Vidal, D.; Malbrunot, P. Gas Adsorption on Zeolites at High Pressures. *Langmuir* **1996**, *12*, 4190.
(16) Walton, K. S.; Cavalcante, C. L., Jr; LeVan, M. D. Adsorption Equilibrium of Alkanes on a High Surface Area Activated Carbon Prepared from Brazilian Coconut Shells. *Adsorption* **2005**, *11*, 107.
(17) Walton, K. S.; Cavalcante, C. L., Jr; LeVan, M. D. Adsorption of Light Alkanes on Coconut Nanoporous Activated Carbon. *Braz. J. Chem. Eng.* **2006**, *23*, 555.
(18) Malek, A.; Farooq, S. Comparision of Isotherm Models for Hydrocarbon Adsorption on Activated Carbon. *AIChE J.* **1996**, *42*, 11.
(19) Toth, J. *Adsorption Theory, Modeling and Analysis*; Dekker: New York, 2001.
(20) Do, D. D. *Adsorption Analysis: Equilibria and Kinetics*; Imperial College Press: Boston, 1998; Vol. 2.
(21) Myers, A. L. Equation of State for Adsorption of Gases and Their Mixtures in Porous Materials. *Adsorption* **2003**, *9*, 9.
(22) Stoeckli, H. F.; Kraehenbuehl, F.; Ballerini, L.; De Bernardini, S. Recent Developments in the Dubinin Equation. *Carbon* **1989**, *27*, 125.
(23) Mehta, S. D.; Danner, R. P. An Improved Potential Theory Method for Predicting Gas−Mixture Adsorption Equilibria. *Ind. Eng. Chem. Fundam.* **1985**, *24*, 325.